JOURNAL OF MATERIALS SCIENCE 29 (1994) 3733–3737

Synthesis and characterization of $(Sr_{1-x}, K_{2x})Zr_4(PO_4)_6$ ceramics

CHIEN-JEN CHEN, LI-JIAUN LIN, DEAN-MO LIU*
Materials Research Laboratories, Industrial Technology Research Institute, Hsingchu, Chutung, 31015, Taiwan

Single phase $(Sr_{1-x}, K_{2x})Zr_4(PO_4)_6$, where x lies between 0.0 and 1.0, ceramic powder with a submicron scale particle size has been synthesized successfully at calcination temperatures as low as 650–750 °C by a sol–gel technique. The formation of the powder strongly depends on calcination temperature, but is independent of solution pH in the studied range. Dilatometric measurement shows an ultra-low linear coefficient of thermal expansion of $0.1 \times 10^{-6}\,°C^{-1}$ when $x = 0.5$ at temperature intervals of 25–1000 °C. Thermal conductivity and flexural strength of the materials were determined at ambient temperature to be 1.0 $W m^{-1} K^{-1}$ and as high as 280 MPa, respectively, indicating that this material can be an excellent candidate in many applications, especially those subjected directly to severe environments.

1. Introduction

Since the discovery of materials in the system $Na_{1+x}Zr_2P_{3-x}Si_xO_{12}$ (known as Nasicon), which exhibit a variety of thermal expansion coefficients from positive to near zero and to negative, a new structural family of low thermal expansion materials, designated NZP (sodium zirconyl phosphate which is regarded as the prototype composition of Nasicon) [1–3], has received worldwide attention.

The thermal expansion mechanism of NZP has been explained by a model based on rotation of constituent PO_4 tetrahedra and ZrO_6 octahedra in the lattice [4]. The thermal expansion anisotropy (TEA) caused by opposite crystallographic axial displacement usually limits their applications by the presence of microcracks [5–7]. Fortunately, due to their enrichment in ionic substitution [1], the TEA of the materials can be reduced considerably by incorporating materials having an opposing coefficient of thermal expansion (CTE) such as $(Ca_{1-x}, Mg_x)Zr_4(PO_4)_6$ [8, 9], $(Ca_{1-x}, Sr_x)Zr_4(PO_4)_6$ [10] and $Ba_{1+x}Zr_4P_{6-2x}Si_{2x}O_{24}$ [11]. In spite of having ultra-low CTE and minimum TEA, thermal conductivity data of the aforementioned materials are not available in published papers except for $(Ca_{1-x}, Mg_x)Zr_4(PO_4)_6$ which shows lower thermal conductivity [8, 9] compared to ZrO_2, a conventional leading thermal barrier material.

In this study, new NZP-type materials containing alkali and alkaline-earth elements, termed $(Sr_{1-x}, K_{2x})Zr_4(PO_4)_6$, i.e. SKZP, has been synthesized by the incorporation of potassium instead of some of the strontium in $SrZr_4(PO_4)_6$ [10, 12]. Accordingly, an ultra low CTE resulting from $SrZr_4(PO_4)_6$ and $KZr_2(PO_4)_3$, which possess opposing axial CTE and low thermal conductivity due to increased lattice defects such as vacancies that decreasing the mean free path of thermal waves, are expected. Powder synthesizing parameters, such as solution pH and calcination temperature, and powder characteristics were examined. Thermal expansion and thermal conductivity of the ceramic were also determined.

2. Experimental procedures

2.1. Powder preparation

Single phase SKZP powders were synthesized by a sol–gel process, reagent grade $SrCO_3$ (99.5%), K_2CO_3 (99.5%), $ZrOCl_2.8H_2O$ (99.0%), and H_3PO_4 (85%), which were used as starting materials, were prepared to form 1.0 M aqueous solutions. Zirconium nitrate, and a nitrate solution containing Sr and K ions with desired molar ratios, were mixed first. The phosphate solution was adjusted to pH 9 by ammonium water prior to incorporation in the nitrate solution, which was stirred vigorously. The solution pH was kept in the range 7.0–11.0 by adding ammonium hydroxide until the solution became a gel. The gel was oven dried at 150 °C, and calcined at 400–1100 °C to drive off volatiles, and the resulting powders were examined using an X-ray diffraction analyser (XRD, Philips PW1700) and a scanning electron microscope (SEM, Cambridge Instruments, S-360). The X-ray diffractometer was equipped with a computerized diffractogram analyser to facilitate crystalline phase identification.

2.2. Sintering

After characterization, the single phase SKZP powders were compacted in a stainless steel die under

* Author to whom correspondence should be addressed.

uniaxial pressure of 30 MPa, followed by cold isostatic pressing at 200 MPa for 5 min. The as-pressed pellets, which were 15 mm in diameter and 5 mm in thickness, were sintered at temperatures of 1150–1300 °C with and without the addition of ZnO as a sintering aid. The densities of the as-sintered bodies were determined using Archimedes' method, with water as an immersing medium.

2.3. Characterization

The strength of the SKZP was determined using a four-point bending tester (Instron, Model 1362) with specimen dimensions of $3 \times 4 \times 40\ mm^3$, at a cross-head speed of $0.5\ mm\ min^{-1}$. The outer span was 30 mm and inner span, 10 mm. Five specimens were used for each measurement. The specimens used for thermal expansion measurement were prepared cylindrically with a standard length of 25 mm. The porosity of the specimens was less than 5%. The bulk coefficient of thermal expansion (CTE) of the SKZP was determined from ambient temperature to 1000 °C at $10\ °C\ min^{-1}$ by means of a dilatometer (Netzsch, Model DIL 402E). The thermal conductivity of the material was determined at ambient temperature using a laser flash technique (ULVAC, SINKU-RIKO Inc., Model TC-3000 H M).

3. Results and discussion

3.1. Effect of solution pH

Fig. 1 illustrates the X-ray diffraction patterns of the resultant powders for $x = 0.5$ obtained at various solution pHs followed by calcining at 1100 °C for 10 h. SKZP precipitates as a single phase solid solution in all the studied pHs, i.e. from pH 7 to pH 11, however, it seems difficult to form a single phase material below pH 6 (not shown), indicative of an alkaline aqueous solution favouring single phase SKZP formation; which was also seen in other NZP-type materials [9].

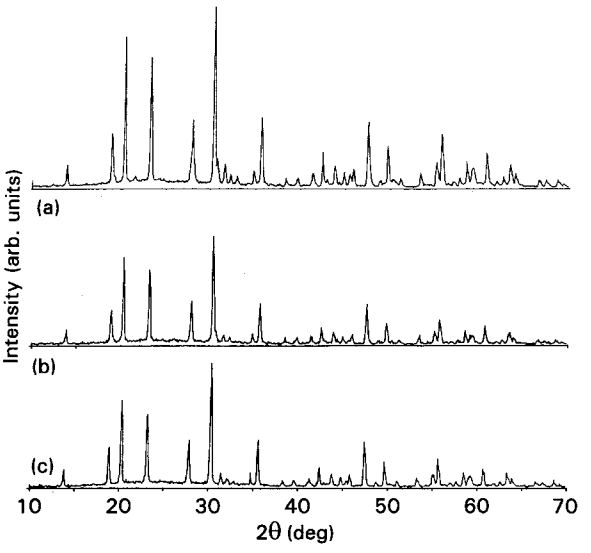

Figure 1 X-ray diffraction patterns of SKZP ($x = 0.5$) at: (a) pH = 7.0, (b) pH = 9.0, and (c) pH = 11.0 (powder prepared at 1100 °C, for 10 h).

The XRD pattern of the single phase SKZP closely resembles those of $SrZr_4(PO_4)_6$ and $KZr_2(PO_4)_3$, according to file Nos 33–1360 and Nos 25–1206 of the Joint Committee on Powder Diffraction Standards [13], respectively, Fig. 2. It is thus realized that potassium can substitute for the strontium position in the framework structure, giving rise to a whole range of solid solutions, and this finding seems to agree well with the model proposed by Lenain *et al.* [4]. The SKZP ceramic is isostructurally related to the NZP material, which has a hexagonal structure with PO_4 tetrahedra and ZrO_6 octahedra linked by corners to form a strong three-dimensional network.

3.2. Effect of calcination temperature and time

Fig. 3 illustrates the X-ray diffraction results of the powder (with $x = 0.5$) calcining at temperatures of 400–1100 °C for 10 h. The phase transforms from amorphous (Fig. 3a) to well crystallized SKZP (Fig. 3d) at about 750 °C, and the lowest temperature

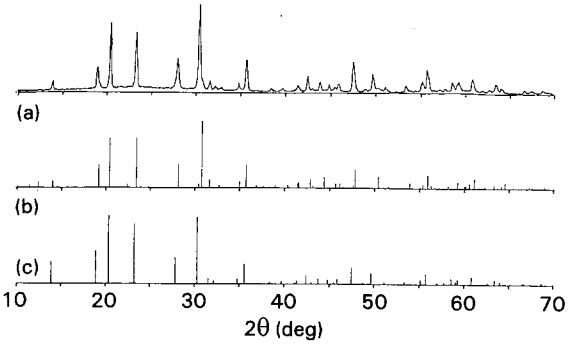

Figure 2 X-ray diffraction of (a) SKZP ($x = 0.5$) compared with the stored standard powder patterns of (b) $SrZr_4(PO_4)_6$, and (c) $KZr_2(PO_4)_3$.

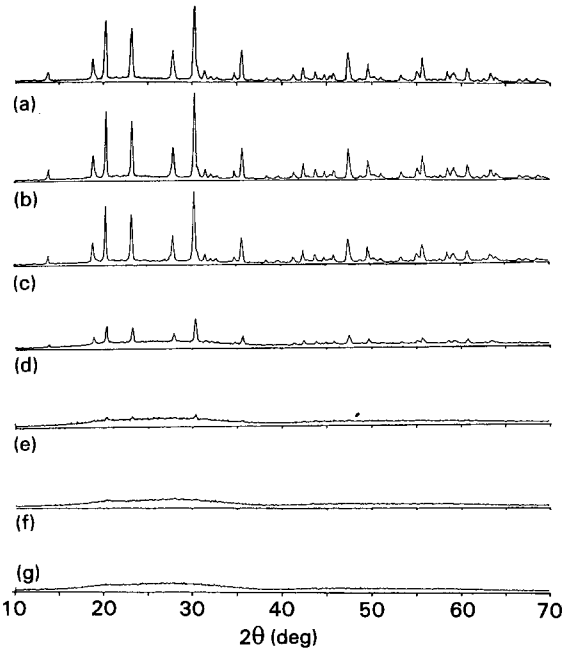

Figure 3 Effect of calcination temperature on the formation of single phase SKZP: (a) 400 °C, (b) 650 °C, (c) 700 °C, (d) 750 °C, (e) 850 °C, (f) 950 °C, and (g) 1100 °C.

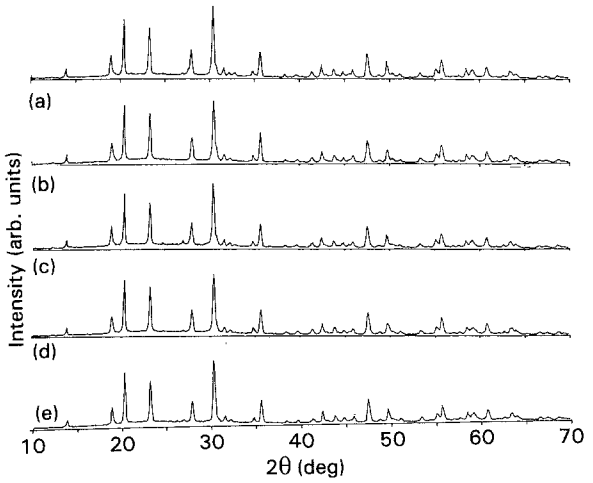

Figure 4 Effect of calcination time on SKZP formation at 850 °C: (a) 0.5 h, (b) 1 h, (c) 3 h (d) 5 h, and (e) 10 h.

for single phase SKZP ceramic formation appears to fall between 650 and 750 °C. The transformation of SKZP is strongly dependent on the temperature, however, it appears that time is almost irrelevant as depicted in Fig. 4, where SKZP with $x = 0.5$ was formed at 850 °C after only 30 min or less. Fig. 5 illustrates scanning electron micrographs of the SKZP particle prepared at different temperatures. The particle size and shape appear to be temperature independent, and an average size of about 0.1 μm at 750 °C can be reached; nevertheless, severe powder agglomeration seems to occur at temperatures below approximately 950 °C (Fig. 5a, b). Necking phenomena occur as a result of calcination at higher temperatures, in Fig. 5c, d, and may strongly decrease powder packing ability and, in consequence, sinterability. The particle size distribution apparently seems to become more uniform and more spherical in shape at lower calcination temperatures.

3.3. Density and strength

Fig. 6 demonstrates the variation of density in terms of different sintering temperatures after 2 h firing without ZnO addition, and at half-hour firing with ZnO. Without the addition of ZnO, the density of the as-sintered compacts increases slightly with increasing temperature, but is still low even up to 1300 °C. However, the density can be improved up to 92% theoretical density (estimated to be 3.25 g cm^{-3}) by employing 1 wt% ZnO. A near-full dense SKZP ceramic can be attained while adding 2 wt% ZnO in a very short period of firing, at temperatures of 1150–1300 °C. The difficulty in sintering the SKZP ceramic may result from large strontium and potassium ions limiting mass diffusion in the lattice, e.g. as observed in the $(Ca, Mg)Zr_4(PO_4)_6$ system [14].

The four-point bending strength varies with density up to 280 MPa at near-full dense material with 3 wt% ZnO, Fig. 7, which exhibits the highest strength among NZP-type materials [5, 6]. The strength, as well

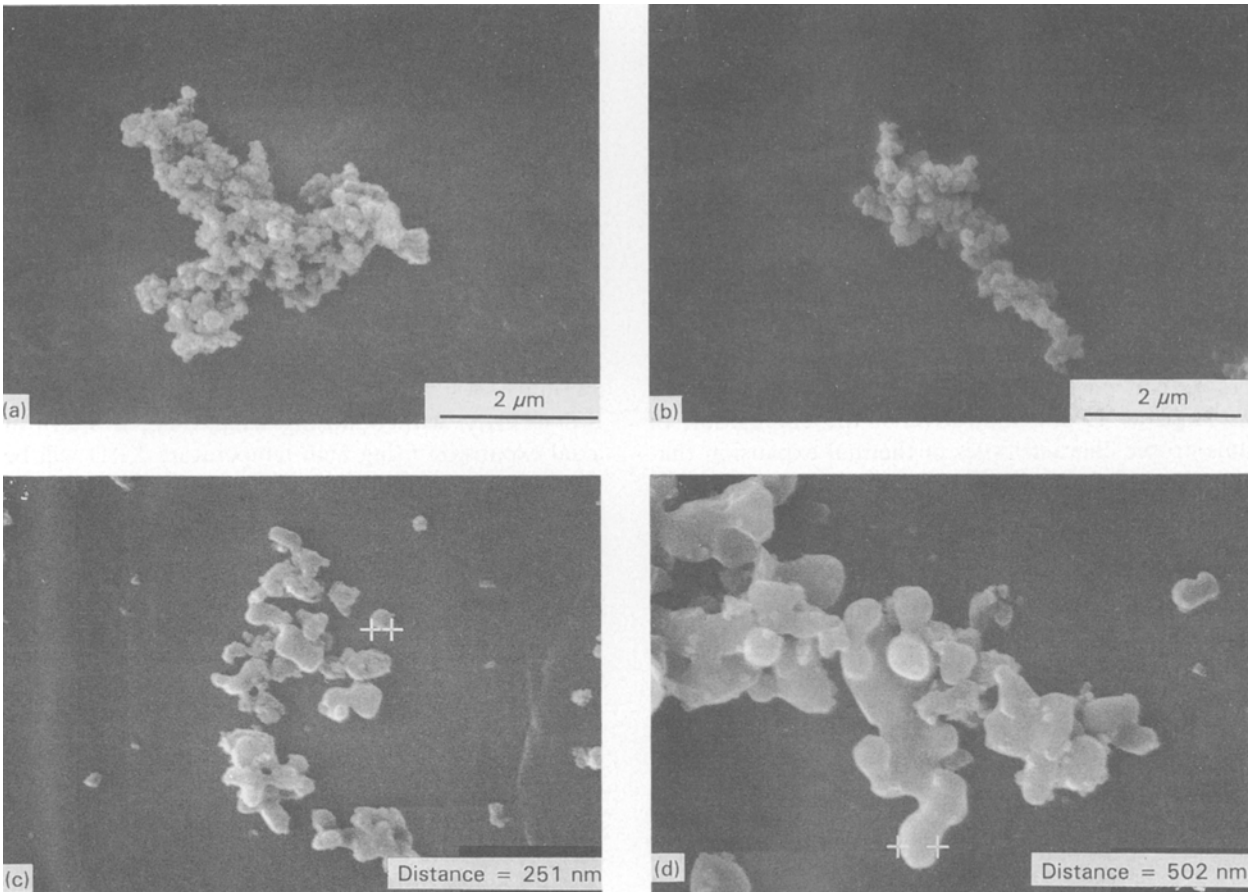

Figure 5 Scanning electron micrographs of the SKZP powder at different calcination temperatures: (a) 750 °C, (b) 850 °C, (c) 950 °C, and (d) 1100 °C.

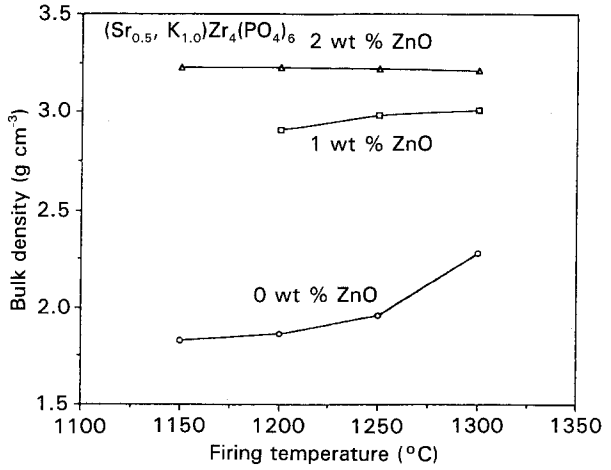

Figure 6 Variation of density in terms of different firing temperatures at various ZnO contents.

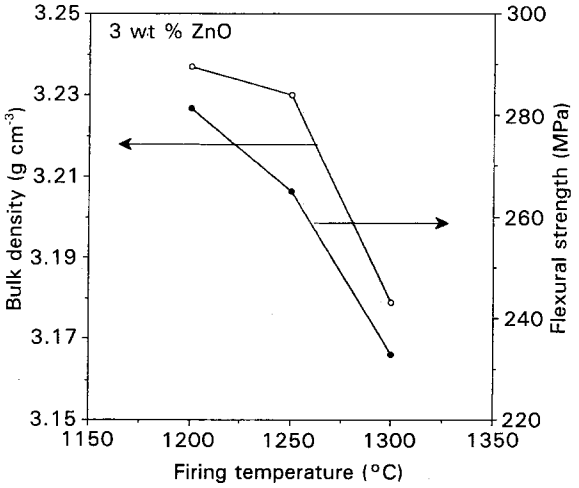

Figure 7 Strength of SKZP with corresponding bulk density at various firing temperatures.

as the density, decreases with increasing sintering temperature suggesting the occurrence of pore coalescence due to oversintering. Fracture surface observation of the SKZP ($x = 0.5$) ceramic, Fig. 8, indicates a transgranular fracture mode that dominates the fracture behaviour. More important, no visible microcracks can be seen in the fracture surface at grains as large as 15 μm, indicative of the elimination of anisotropic characteristics in thermal expansion that usually appear in the relevant materials [8, 10].

3.4. Thermal expansion–thermal conductivity

Thermal expansion behaviour of the SKZP ceramics is shown in Fig. 9, with $x = 0.0$, 0.2, 0.5, 0.8 and 1.0. Two end compounds, $SrZr_4(PO_4)_6$ and $KZr_2(PO_4)_3$, exhibit opposing bulk coefficients of thermal expansion (CTE), i.e. $3.1 \times 10^{-6}\,°C^{-1}$, and $-1.2 \times 10^{-6}\,°C$ respectively. The bulk CTE, however, can be minimized by incorporating two end compositions with appropriate ratios, such as those found in $(Ca_{1-x}, Mg_x)Zr_4(PO_4)_6$ [7, 8] and $(Ca_{1-x}, Sr_x)Zr_4(PO_4)_6$ [9] ceramics where ultra-low CTE and low thermal expansion anisotropy (TEA) were observed at $x = 0.4$ for the former and at $x = 0.25$ for the latter.

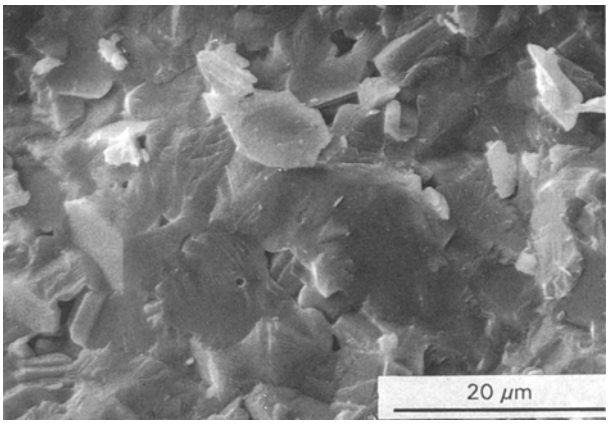

Figure 8 Fracture surface of SKZP ceramics, which shows a transgranular fracture mode.

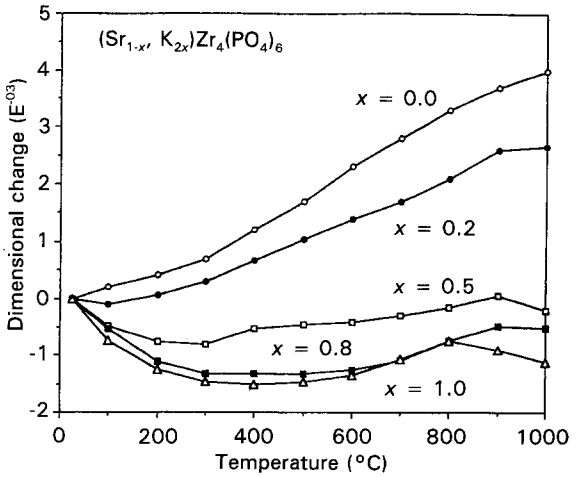

Figure 9 Thermal expansion behaviour of SKZP ceramics for various x values.

The influence of porosity on CTE values is negligible [7], the thermal expansion behaviours in Fig. 8 can, therefore, be regarded as those of the dense phase. The CTEs vary from positive values when $x < 0.5$ to negative values when $x > 0.5$, and become near zero at $x \approx 0.5$. The occurrence of near zero CTE at $x = 0.5$ suggests the near complete annihilation of axial expansion in the lattice, since it consists of equivalent amounts of material, i.e. $SrZr_4(PO_4)_6$ and $KZr_2(PO_4)_3$, with opposing axial CTE, a study of axial expansion using high temperature XRD will be reported elsewhere [15].

The thermal conductivity of the SKZP ceramic was determined using a laser flash technique at $1\,W\,m^{-1}\,K^{-1}$, which is lower than that of ZrO_2, about $2\,W\,m^{-1}\,K^{-1}$, at ambient temperature and is comparable with several well known NZP-type ceramics $(Ca_{1-x}, Mg_x)Zr_4(PO_4)_6$ [9] and $(Ca_{1-x}, Sr_x)Zr_4(PO_4)_6$ [16]. The lower thermal conductivity of SKZP may result from the formation of lattice defects, such as oxygen vacancy and/or positive ion vacancy, which act as a scattering centre for thermal waves, due to ion substitution [17].

4. Conclusions

Single phase $(Sr_{1-x}, K_{2x})Zr_4(PO_4)_6$ powder has been

synthesized successfully via a gel technique at calcination temperatures as low as 650–750 °C. The powder obtained shows an average particle size varying from about 0.1–0.5 μm, and has an uniform distribution in size and shape. The SKZP ceramic exhibits flexural strength as high as 280 MPa, a near zero bulk coefficient of thermal expansion, i.e. $0.1 \times 10^{-6}\,°C^{-1}$, while $x = 0.5$, and a low value of thermal conductivity, which makes the material an excellent candidate for application in severe environments, especially for thermal insulating applications.

Acknowledgements

The authors wish to give their grateful acknowledgement to the Ministry of Economic Administration, Republic of China for supporting this work.

References

1. J. ALAMO and R. ROY, *J. Mater. Sci.* **21** (1986) 444.
2. R. ROY, D. K. AGRAWAL, J. ALAMO and R. A. ROY, *Mater. Res. Bull.* **19** (1984) 471.
3. G. E. LENAIN, H. A. McKINSTRY, S. Y. LIMAYE and A. WOODWARD, *J. Mater. Sci.* **19** (1984) 1451.
4. G. E. LENAIN, H. A. McKINSTRY, J. ALAMO and D. K. AGRAWAL, *J. Mater. Sci.* **22** (1987) 17.
5. I. YAMAI and T. OOTA, *J. Amer. Ceram. Soc.* **70** (1987) 585.
6. *Idem., ibid.* **68** (1985) 273.
7. D. M. LIU and J. J. BROWN, *Mater. Chem. Phys.* **33** (1993) 43.
8. S. M. VAN AKEN, MS Thesis, Virginia Polytechnic Institute and State University (1990).
9. J. J. BROWN, D. HIRSCHFELD, D. M. LIU, Y. YANG, T. LI, R. E. SWANSON, S. VAN AKEN and J. M. KIM, US Patent No. 5 102 836, April 1992.
10. S. Y. LIMAYE, D. K. AGRAWAL, H. A. McKINSTRY and R. ROY, US Patent No. 4 801 566, January 1989.
11. D. P. STINTON, *Ceram. Technol. Newslett.* **35** (1992) 7.
12. S. Y. LIMAYE, D. K. AGRAWAL and H. A. McKINSTRY, *J. Amer. Ceram. Soc.* **70** (1987) C232.
13. Joint Committee on Powder Diffraction Standards (JCPDS),International Centre for Diffraction Data, Swarthmore, PA.
14. D. M. LIU, *J. Mater. Sci.* **28** (1993) 6353.
15. D. M. LIU, L. J. LIN and C. J. CHEN, *J. Appl. Crystallog.* in press.
16. D. M. LIU, Unpublished work.
17. D. M. LIU, C. J. CHEN and L. J. LIN, *J. Appl. Phys.* **75** (1994) 3765.

Received 22 June 1993
and accepted 28 January 1994